

## Original Full Length Article

## Modeling of cortical bone adaptation in a rat ulna: Effect of frequency

N. Chennimalai Kumar, J.A. Dantzig, I.M. Jasiuk\*

Department of Mechanical Science and Engineering, University of Illinois at Urbana-Champaign, 1206 West Green Street, Urbana, IL 61801, USA

## ARTICLE INFO

## Article history:

Received 12 July 2011

Revised 11 December 2011

Accepted 13 December 2011

Available online 22 December 2011

Edited by: David Fyhrie

## Keywords:

Poroelasticity

Dissipation energy

Interstitial fluid flow

Cortical bone adaptation

Finite element modeling

Evolution law

## ABSTRACT

We employ a recently developed model for the adaptation of cortical bone in response to mechanical loading to study the effect of loading frequency on the computed response, and we compare our results to previous experimental measurements on rat ulnae. We represent the cortical bone as a poroelastic material with orthotropic permeability. Bone adaptation in the model is related to a mechanical stimulus derived from the dissipation energy of the poroelastic flow induced by deformation. We account for a non-locality in the mechanotransduction of osteocytes present in the lacunae by using a “zone of influence.” Calculations are done using the finite element method applied to a rat ulna whose geometry is obtained from micro-computed tomography images. We show that the change in the second moment of inertia of the cross-section increases non-linearly and saturates at higher frequency range. The numerical results are then compared quantitatively to experimental data from the literature. Finally, we examine the role of local narrowing of intramedullary canal in our specific ulna in the development of local irregularities in growth.

© 2011 Elsevier Inc. All rights reserved.

## Introduction

Bone responds to mechanical stimulation through adaptation [1–3], which is manifested internally in trabecular bone, and externally in cortical bone. Dynamic mechanical stimulus, usually applied as cyclic loading, is essential for adaptation to occur [4–7]. Numerous experimental studies have established that the adaptation response varies with the magnitude of loading [6–8], time dependent parameters such as frequency of loading [9], number of load cycles [5,8–10], and bouts of loading [11,12]. In human cortical bone, adaptation becomes observable for loading frequencies greater than 0.5 Hz [13], increases linearly with frequency in the 1 Hz–10 Hz range [9], after which the adaptation response becomes saturated [10].

Our overarching goal has been to develop a numerical model to predict cortical bone adaptation, and in particular to account for the effect of various loading parameters, discussed above, on the adaptation response. In a previous article [14], we used the strain energy density as a stimulus to trigger adaptation in the model, and used it to examine the effect of the magnitude and temporal bouts of loading on the adaptation behavior. As part of that work, we developed a numerical framework that predicts the growth of cortical bone by first performing a finite element analysis of the deformation within the bone, then computing the mechanical stimulus, and finally using the stimulus to model the adaptation of the cortical bone. However, the strain energy density cannot be used to explain frequency response of bone adaptation, for example the

experimental observation that a fixed number of load cycles applied at increasing frequencies produces a response that at first increases, then saturates at some frequency. This phenomenon can be included by treating the bone as a poroelastic material [15]. In a follow-up article [16], we introduced a stimulus derived from the dissipation energy of the poroelastic flow induced by deformation, and demonstrated the concept on a cyclically loaded rectangular beam. The goal of the work described here is to determine how well the model with poroelastic material characterization can explain the results of frequency sensitivity in an animal model by comparing our computed results with experimental data obtained from the literature. To that end, we integrate the dissipation energy stimulus into our numerical framework in order to simulate the effect of loading frequency on the cortical bone adaptation. We demonstrate the approach using the same rat ulna as in our previous study [14], and verify that the dissipation energy based growth model predicts response that is consistent with previous experimental observations of bone remodeling. We note that this is not a validation of the model, which would require extensive experimental measurements of fluid flow within the bone, which is beyond the scope of the present work.

Load-induced fluid flow in cortical bone has been observed and analyzed by a number of researchers, for example [17–21]. Fritton and Weinbaum's extensive review [22] provides a comprehensive description of the fluid flow-induced mechanotransduction in cortical bone. The trigger for mechanotransduction has been hypothesized to be due to the load-induced fluid flow on the osteocytes [23–25]. It was found that the fluid shear stress and drag force on the osteocyte process tethering fibers can amplify the macroscale strains by more than 50 times [25]. The strain amplification factor was shown to vary non-linearly with respect to loading frequency.

\* Corresponding author. Fax: +1 217 244 6534.

E-mail address: [ijasiuk@illinois.edu](mailto:ijasiuk@illinois.edu) (I.M. Jasiuk).

This paper is organized as follows: we first describe briefly the implementation of the growth algorithm and the development of the dissipation energy based stimulus. The main contribution of this work is to apply the growth algorithm with the dissipation energy stimulus to a finite element model of an actual rat ulna, obtained from serial CT sections. We present the results for a baseline growth simulation, with parameters corresponding to experimental data [11], and compare quantitatively the numerical results to these experimental measurements, and interpret them in terms of cortical bone mechanotransduction. Finally, we examine the role of peculiarities in the geometry of our specific bone in the development of local irregularities in growth.

**Methods**

The construction of the finite element mesh, and the adaptation algorithm were presented in detail in our previous work [14]. We therefore include here only a brief description of the approach, in the interest of making his article self-contained, and refer the interested reader to the original work.

*Finite element model and adaptation algorithm*

We constructed a three-dimensional finite element mesh of the rat ulna by developing a surface model using micro-CT images (obtained with 10 μm resolution) of the ulna cross-sections, and employing the commercial meshing software Hypermesh. The FE mesh, shown in Fig. 1, consists of 62,782 nodes and 37,949 parabolic tetrahedral elements. The experimental conditions used by [11], where 9 N loading at 2 Hz for 360 cycles was applied on the rat ulna in a single bout, were used as the base case for the numerical model for calibration purposes. The adaptation procedure was implemented by displacing the surface nodes along the normal direction based on the following growth law [26,27]:

$$\frac{db_i}{dT} = \begin{cases} A(\phi_i - \phi_{ref}), & \phi_i \geq \phi_{ref} \\ 0, & \text{otherwise} \end{cases} \quad (1)$$

where  $b_i$  is the normal displacement of a node  $i$  (located on the surface over which growth occurs),  $A$  is a proportionality constant,  $\phi_i$  is the local value of the stimulus,  $\phi_{ref}$  is the reference stimulus, and  $T$  is time of growth. Since resorption was not observed in experiments [11], we specifically excluded it from the model. The adaptation algorithm started with a poroelastic stress analysis on the FE model of the rat ulna. The local values of the stimulus at the surface nodes were then computed, and the surface nodes were displaced according to Eq. (1). A FE analysis was performed on the updated model, and the cycle was continued until convergence (i.e., the surface displacements are zero) or until a specified number of growth time steps have been completed. The procedure is explained in detail in our earlier paper [14].

*Development of the dissipation energy stimulus*

Cortical bone has porosities at several different structural scales. They include vascular (canal network), lacuno-canalicular, and collagen-apatite porosities [15]. Osteocytes, which are housed in the lacunae, have been shown to be responsible for mechanotransduction in previous experimental and analytical studies. The load induced fluid flow can occur at the canal network and the lacuno-canalicular

porosities [15]. These porosities are illustrated for mouse bones by [28]. Rat ulna exhibits similar tortuous canal paths [29]. For simplicity, we model the cortical bone as a homogenized poroelastic material, with the poroelastic properties accounting for the canal network and lacuno-canalicular porosities. The intramedullary canal, which is at a higher scale, is treated as a source for fluid to move freely into and out of the cortical bone.

The theory of poroelasticity is well known in the literature [15,30–32], and we provide here just a short overview of poroelastic fundamentals for clarity of exposition in the work that follows. We treat the bone as a saturated poroelastic medium, whose deformation is governed by the following pair of equations:

$$2G\epsilon_{ij} = \sigma_{ij} - \left(\frac{\nu}{\nu+1}\right)\sigma_{kk}\delta_{ij} + \alpha\left(\frac{1-2\nu}{1+\nu}\right)p\delta_{ij}; \quad 2G\zeta = \alpha\left(\frac{1-2\nu}{1+\nu}\right)\left(\sigma_{kk} + \frac{3p}{B}\right). \quad (2)$$

where we have introduced the following field variables: stress tensor  $\sigma$ , strain tensor  $\epsilon$ , pore pressure  $p$ , and the variation in fluid content  $\zeta$ . The material parameters are the shear modulus  $G$ , Poisson's ratio  $\nu$ , the Willis coefficient  $\alpha$ , and Skempton's coefficient  $B$ .  $\delta_{ij}$  is the Kronecker delta, and  $i, j = 1, 2, 3$  represent coordinate directions. The fluid mass flow rate  $q_i$  is computed from the pressure using Darcy's law,

$$q_i = -\kappa_{ij} \frac{\partial p}{\partial x_j}, \quad (3)$$

where  $\kappa_{ij}$  is the orthotropic hydraulic permeability tensor ( $\kappa_{ij} = k_{ij}/\mu$ , where  $k_{ij}$  is the orthotropic intrinsic permeability and  $\mu$  is the dynamic viscosity of the fluid). The mass flow rate is related to the fluid velocity  $v_i^f$  as  $q_i = \rho_f n_p v_i^f$ , where  $\rho_f$  is the density of the fluid and  $n_p$  is the porosity.

Inserting the constitutive equations (Eq. (2)) and Darcy's law (Eq. (3)) into the mass and momentum balance equations, and non-dimensionalizing the length and time scales lead to the following equation for the evolution of the pore pressure:

$$\nabla^2 \left(\sigma_{kk} + \frac{3p}{B}\right) = Fo \frac{\partial}{\partial T^*} \left(\sigma_{kk} + \frac{3p}{B}\right), \quad (4)$$

$\mathbf{X}^* = \mathbf{x}/d$  ( $d$  is a characteristic length),  $T^* = \omega t$ , and  $Fo = \omega d^2/c$  is the Fourier number, which represents the ratio of the timescale for hydraulic diffusion ( $d^2/c$ ) to the timescale of the applied load ( $1/\omega$ ). Here  $c$  is the hydraulic diffusivity, which is proportional to the intrinsic permeability.

We choose as a characteristic measure of the growth stimulus the dissipation potential of the viscous fluid flow  $\varphi$ , defined as,

$$\varphi = -n_p \mathbf{v}^f \cdot \nabla p = \frac{1}{2} (n_p \mathbf{v}^f) \cdot \boldsymbol{\kappa}^{-1} \cdot (n_p \mathbf{v}^f), \quad (5)$$

where  $n_p$  is the porosity,  $\mathbf{v}^f$  is the fluid velocity, and  $\boldsymbol{\kappa}$  is the permeability tensor [16]. The stimulus applied in the growth adaptation model is the time integral over the time period of loading of the dissipation potential.

We introduce a “zone of influence,” shown schematically in Fig. 2, over which the stimulus is averaged, to model a non-local behavior. This represents a collective contribution to growth from neighboring osteocytes, which can communicate through the processes inside the canalicular space. The final form of the dissipation energy stimulus is given by:

$$\varphi = \frac{\int_V \left( \int_0^t \frac{1}{2} n_p \mathbf{v}^f \cdot \boldsymbol{\kappa}^{-1} \cdot n_p \mathbf{v}^f dt \right) f(\|\mathbf{x}\|) dV}{\int_V f(\|\mathbf{x}\|) dV}, \quad (6)$$

where  $V$  is the volume of the zone of influence,  $f$  is an influence function, and  $t$  is the total time period of loading. Following the results of our earlier study [16], we defined  $f(\|\mathbf{x}\|) = (\|\mathbf{x}\|/R)^3 e^{-11\|\mathbf{x}\|/R}$ , where  $R$  is a characteristic length, in this case 0.8 mm, the approximate thickness of the ulna, in

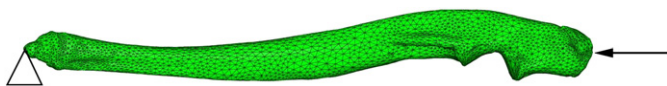


**Fig. 1.** Finite element model of the rat ulna consisting of 62,782 nodes and 37,979 parabolic tetrahedral elements.

Download English Version:

<https://daneshyari.com/en/article/2779672>

Download Persian Version:

<https://daneshyari.com/article/2779672>

[Daneshyari.com](https://daneshyari.com)